JACS Au
AN OPEN ACCESS JOURNAL OF THE AMERICAN CHEMICAL SOCIETY

pubs.acs.org/jacsau
Article

Synthesis of Protoberberine Alkaloids by C−H Functionalization and Anionic Aza-6π-Electrocyclization: Dual Activity as AMPK Activators and Inhibitors

Yujie Cao, Justin S. M. Perry,[#] Eryun Zhang,[#] Andy Trinh, Arnav Kacker, Shayne Cruz, Hannah Ceballos, Aaron Pan, Wendong Huang,* and Kevin G. M. Kou*

Cite This: JACS Au 2025, 5, 1429−1438

Read Online

ACCESS | Metrics & More | Article Recommendations | Supporting Information

ABSTRACT: 5′-Adenosine monophosphate-activated protein kinase (AMPK) plays a critical role in maintaining cellular energy homeostasis, and its activation has garnered attention for treating chronic metabolic diseases. Inhibitors of AMPK are underdeveloped but bear implications in treating cancers, controlling autophagy, and elderly wasting. Protoberberine alkaloids are typically regarded as AMPK activators. Herein, we report a modular synthesis strategy to access a collection of oxyberberine alkaloids, including the first synthesis of stepharotudine. In vitro assays reveal how subtle structural modifications can negate AMPK activation while conferring unprecedented inhibitory properties within the same class of compounds, which was previously unknown. Key steps in the synthesis include an oxidative Rh(III)-catalyzed C−H functionalization using electron-rich alkenes, NaH-mediated reductive *N*−O bond cleavage, and a rare example of an anionic aza-6π-electrocyclization. Additionally, we provide mechanistic support for nucleophilic hydride transfer reactivity with NaH in DMF.

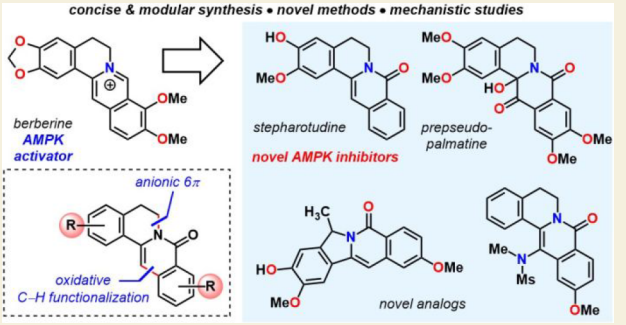

KEYWORDS: *protoberberines, C−H functionalization, aza-electrocyclization, anionic 6π, AMPK, AMPK inhibition*

1. INTRODUCTION

Lifestyles that emphasize exercise and caloric restriction effect an increase in the activity of 5′-adenosine monophosphate-activated protein kinase (AMPK), a key regulator of metabolic and energy homeostasis.[1] This favorable enhancement curtails risks in developing chronic metabolic diseases like type-2 diabetes, obesity, nonalcoholic fatty liver disease (NAFLD), nonalcoholic steatoheptatitis (NASH), and cancers, even decelerating the aging process. As such, targeting AMPK is emerging as a promising avenue for therapeutic intervention—the aim being to emulate the low energy state that is conducive to combating diseases arising from the destabilizing imbalance between nutrient intake (i.e., high-calorie diets) and energy expenditure (i.e., increasingly sedentary routines).[2] Nearly all research efforts have focused on developing activators of AMPK, while their corresponding inhibitors remain underexplored. In fact, there are instances where AMPK promotes tumor cell survival and that its deficiency represses tumor growth.[2d,3] Therefore, the ability to regulate AMPK levels, including its inhibition, can have important implications for advancing cancer treatments. Controlling AMPK can also be developed into a strategy for modulating autophagy, a metabolic process that degrades damaged organelles and is associated with a wide variety of diseases.[4]

In contrast to the relatively abundant number of synthetic molecules and natural products that act as AMPK activators,[5] there are only three compounds known to inhibit AMPK,[3b] all of which are multikinase inhibitors (Figure 1a). The Huang lab has a longstanding interest in understanding the mechanisms that underlie the therapeutic effects of AMPK modulators such as metformin and berberine (**1**, Figure 1a), and have uncovered a novel link between intestinal AMPK activation and brown adipose tissue (BAT) thermogenic regulation that is accompanied by modulation of the antimicrobial peptide (AMP)-controlled gut microbiota.[2c] Given how metabolic intermediates of berberine are similarly bioactive or may be the active forms following oral administration,[6] we hypothesized that the rarer biosynthetic precursors of berberine, such as prepseudopalmatine (**2**), 8-oxypseudopalmatine (**3**), and stepharotudine (**4**) could also exert AMPK modulation activity. Unlike berberine, protoberberine alkaloids resembling

Received: January 15, 2025
Revised: February 20, 2025
Accepted: February 21, 2025
Published: February 27, 2025

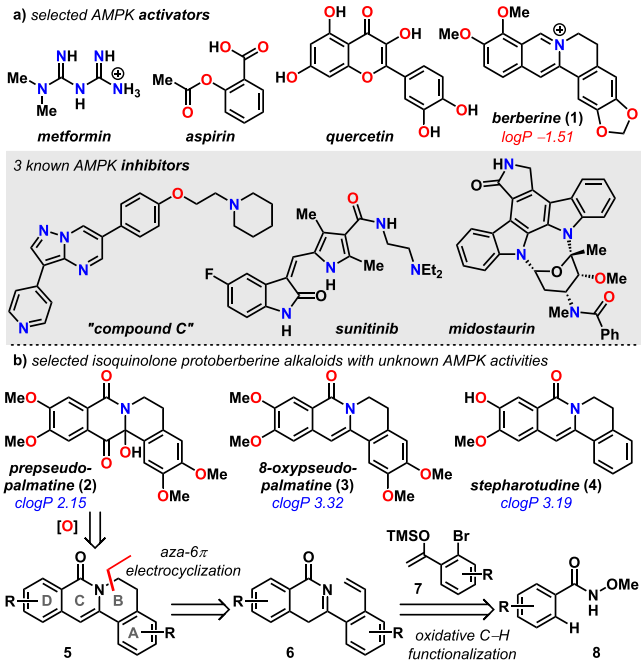

Figure 1. (a) Examples of AMPK modulators. (b) Our synthesis approach to protoberberine alkaloids with unknown AMPK activities.

2–**4** make up minor components of the *Magnoliaceae*, *Ranunculaceae*, *Berberidaceae*, and *Menispermaceae* families of plants and are not accessible to the biomedical community. We have thus devised a convergent strategy to prepare natural and unnatural protoberberine analogs de novo highlighting methodologies developed in the Kou lab. The strength of this synthesis strategy compared to others[7] lies in its modularity in enabling derivatization of all four rings within the protoberberine scaffold. Compounds **2**–**4** and their derivatives were envisioned to arise from tetracyclic intermediate **5**. We imagined disconnecting ring B of the tetracycle through a novel aza-6π-electrocyclic transform, thus simplifying the structure to dihydroisoquinolone **6**, which can be assembled directly from silyl enol ether **7** and hydroxamic ester **8** by oxidative C–H functionalization. This strategy led to the preparation of 13 protoberberine-type alkaloids to survey the structure–activity relationship (SAR) with respect to AMPK modulation. We found that the absence of the cationic charge imposed by the quaternized nitrogen (i.e., berberine) stymies AMPK activation ability, and the neutral protoberberines synthesized in this study represent novel examples of AMPK inhibitors.

2. RESULTS AND DISCUSSION

2.1. Synthesis of Protoberberine Alkaloids

To achieve a concise and modular synthesis strategy, we integrated an oxidative Rh(III)-catalyzed C–H functionalization (see SI) previously developed in the Kou lab that combines densely substituted enol silanes **7** with hydroxamic esters **8** to produce densely substituted 3-hydroxydihydroisoquinolones **9**, which upon treatment with aqueous HCl, eliminate water to form isoquinolones **10a**–**k** in 24–76% yields after two steps (Scheme 1a).[8] Given the multisubstitution patterns of the compound precursors, which are more complex than those reported in the original study, the reactivity and modest yields are remarkable. Our pursuit of oxidative C–H functionalization with enol silanes solves a major limitation in alkyne reactivity: enol silanes **7** are surrogates for terminal alkynes, which are poorly precedented in C–H functionalization,[9,10] with the exception of a recent study by the Pfizer Oncology group demonstrating success with propyne.[11] This methodology was effective in introducing multiple substitution patterns, including a bromide functional handle, into rings A and D. A ligand-free palladium-catalyzed cross-coupling was optimized to append a vinyl group, generating styrene derivatives **11** in up to 98% yields. The presence of an aldehyde in aryl bromide **10b** hampers productive cross-coupling, whereas aldoxime **10c** undergoes competitive palladium-catalyzed aldoxime rearrangement,[12] generating benzamide side-product **11c′** (37%) alongside the target Suzuki product (25%). These reactions set the stage for *N*-deprotection coupled to a novel anionic 6π-aza-electrocyclization. This process bypasses an otherwise multistep hydroboration/oxidation/activation/cyclization sequence[13] and directly furnishes the tetracyclic alkaloid core in 20–84% yields (Scheme 1b). The use of NaH in DMF is critical and substituting the solvent for DMSO or THF shutters reactivity. In contrast to the syntheses of tetramethoxyoxyberberines (**3**) and (**14**) where NaH (3 equiv) mediated a tandem *N*–*O* cleavage[8,14] and aza-6π-electrocyclization in 20 h without additional additives, NaH induced *N*–*O* cleavage but only partial cyclization in all other examples. To circumvent this, we devised a one-pot protocol whereby KO*t*-Bu (0.5 equiv) is added following *N*-deprotection and additionally reacted for 18–22 h to fully convert the reactant and complete the electrocyclization. Moderate to good yields (42–84%) were generally observed when the oxyberberine D-rings were electron-neutral (e.g., **4**, **16**, **17**) or electron poor (e.g., **18**, **19**). In contrast, lower isolated yields (15–31%) were obtained when the D-ring was substituted with electron-donating groups (i.e., **3**, **14**, **20**, **21**). The reduction in yield is attributed to sensitivity of the oxyberberine alkaloids to silica gel and alumina treatments, rather than inefficiencies in the electrocyclization reaction. In all cases, the electrocyclization produces high yields as determined by NMR analysis. Of note, the Suzuki reaction of aryl halide **10f** is accompanied by *N*–*O* cleavage, producing only deprotected isoquinolone **11f′** in 54% yield. Aryl halide **10k** with the three aryl halide bonds decomposes under the reaction conditions and therefore could not be converted to **11k**. In the cases of stepharotudine (**4**) and methoxystepharotudine **20**, their 5-exo-trig cyclization counterparts **4-iso** (2%) and **5-iso** (3%) were also formed as minor side-products and represent B-ring distortion analogs of stepharotudine.[15] Oxidation of 8-oxypseudopalmatine (**3**) led to the first preparation of the naturally occurring prepseudopalmatine (**2**) in 48% isolated yield.

2.2. AMPK Modulation and Structure–Activity Relationship

We initially targeted oxyberberine natural products **2** and **3** with higher oxygenation patterns because they have not been studied in a biological context and **2** had not been synthesized previously. In vitro kinase activity assays using the AMPK (α1/β1/γ1) kinase enzyme system (presented as IC_{50} data) and in vivo assays using the human intestinal epithelial cell line HT29[2c] revealed that altering the cationic isoquinolinium moiety characteristic of berberine (**1**) for the neutral isoquinolone stimies AMPK activation activity (Scheme 1b,c). Highly oxygenated alkaloids **2**, **3**, and **14** were poorly

https://doi.org/10.1021/jacsau.5c00047
JACS Au 2025, 5, 1429–1438

Scheme 1. (a) Concise Synthesis Enabled by (i) Oxidative Rh-Catalysis and (ii) Anionic Aza-6π-Electrocyclization; Conditions: [a][Cp*RhCl$_2$]$_2$ (5 mol %), AgOAc (2.2 equiv), THF (0.2 M), 50 °C, 18 h; [b]PdCl$_2$ (5 mol %), Boroxine (1.5 equiv), K$_3$PO$_4$ (3 equiv), 1,4-Dioxane/H$_2$O (0.1 M), 130 °C, 18 h; [c]% Conv. by ^{1}H NMR; [d]NaH (3 equiv), 130 °C, 20 h; [e]NaH (2 equiv), 130 °C, 3 h, Then KO*t*-Bu (0.5 equiv), 130 °C, 18 h; [f]NaH (3 equiv), 130 °C, 3 h, Then KO*t*-Bu (0.5 equiv), 130 °C, 20 h; (b) IC$_{50}$ Efficacies for AMPK(α1/β1/γ1) and Discovery of Stepharotudine Analogs as Novel AMPK Inhibitors; (c) AMPK Inhibition Assays; IC$_{50}$ Data Are Extracted and Presented with Compounds in Scheme 1b; (d) Western Blot Analysis of Phosphorylated AMPK, Total AMPK, and Glyceraldehyde 3-Phosphate Dehydrogenase; Control = 0.1% DMSO

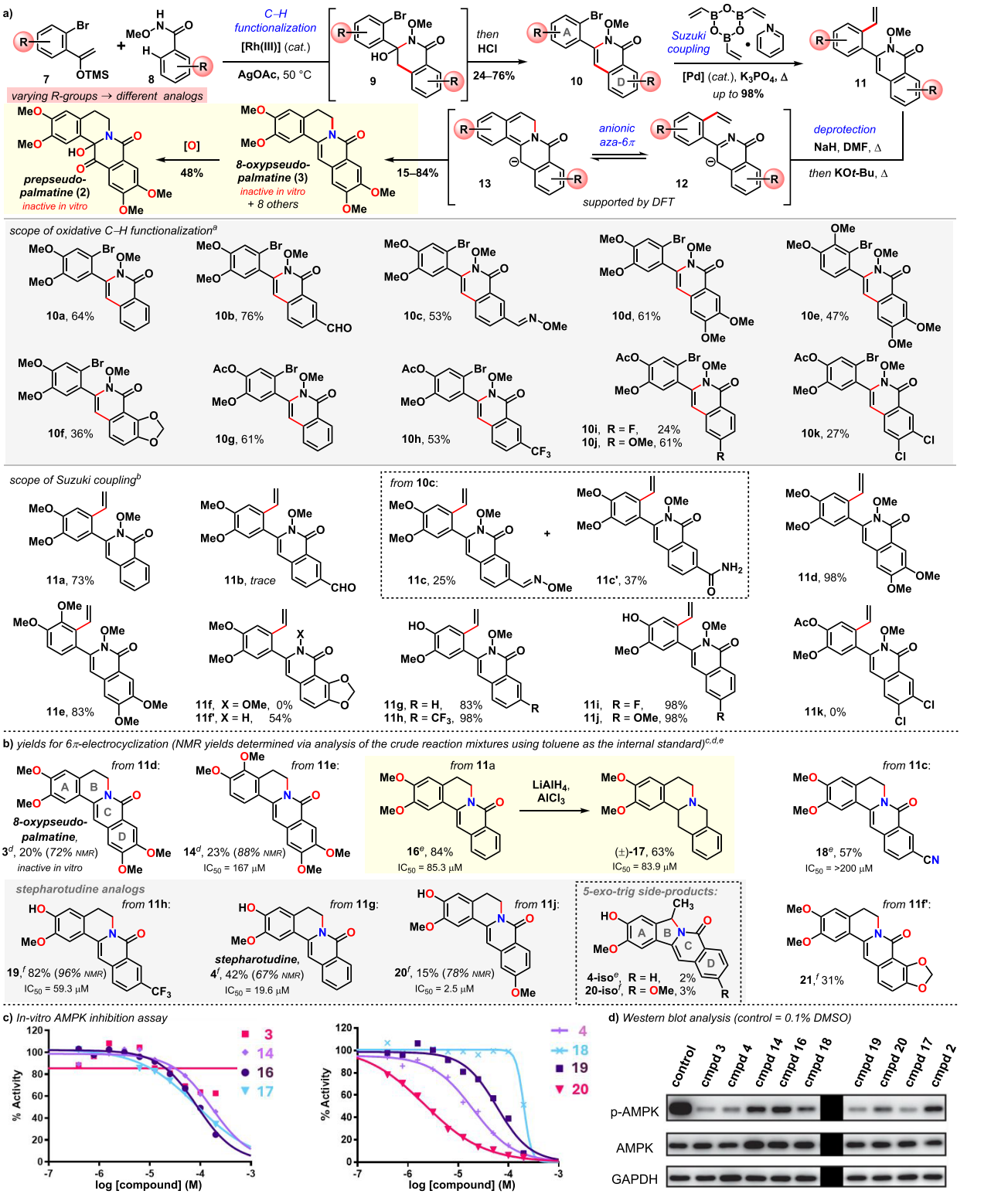

active or inactive in vitro. Removal of the two methoxy groups from the D ring resulted in a compound that inhibited AMPK with an IC$_{50}$ of 85.3 μM. Fully reducing the enaminone motif of the isoquinolone resulted in racemic tertiary amine **17** with

https://doi.org/10.1021/jacsau.5c00047
JACS Au 2025, 5, 1429−1438

Scheme 2. (a) Mechanisms of NaH-Mediated *N*−*O* Cleavage Computed by DFT at the B3LYP/6-311+G(2d,p) Level of Theory with Implicit Solvation (CPCM) by DMF at 428.15 K (See SI for Complete Energy Profiles); Free Energies Expressed in kcal/mol; (b) Chelation-Assisted Nucleophilic Hydride Delivery with Both Implicit (CPCM, DMF) and Explicit Solvation; Methyl Hydrogens Are Omitted for Clarity; (c) Observed Experimental S_NAr Reactivity Consistent with Hydride Transfer Pathway

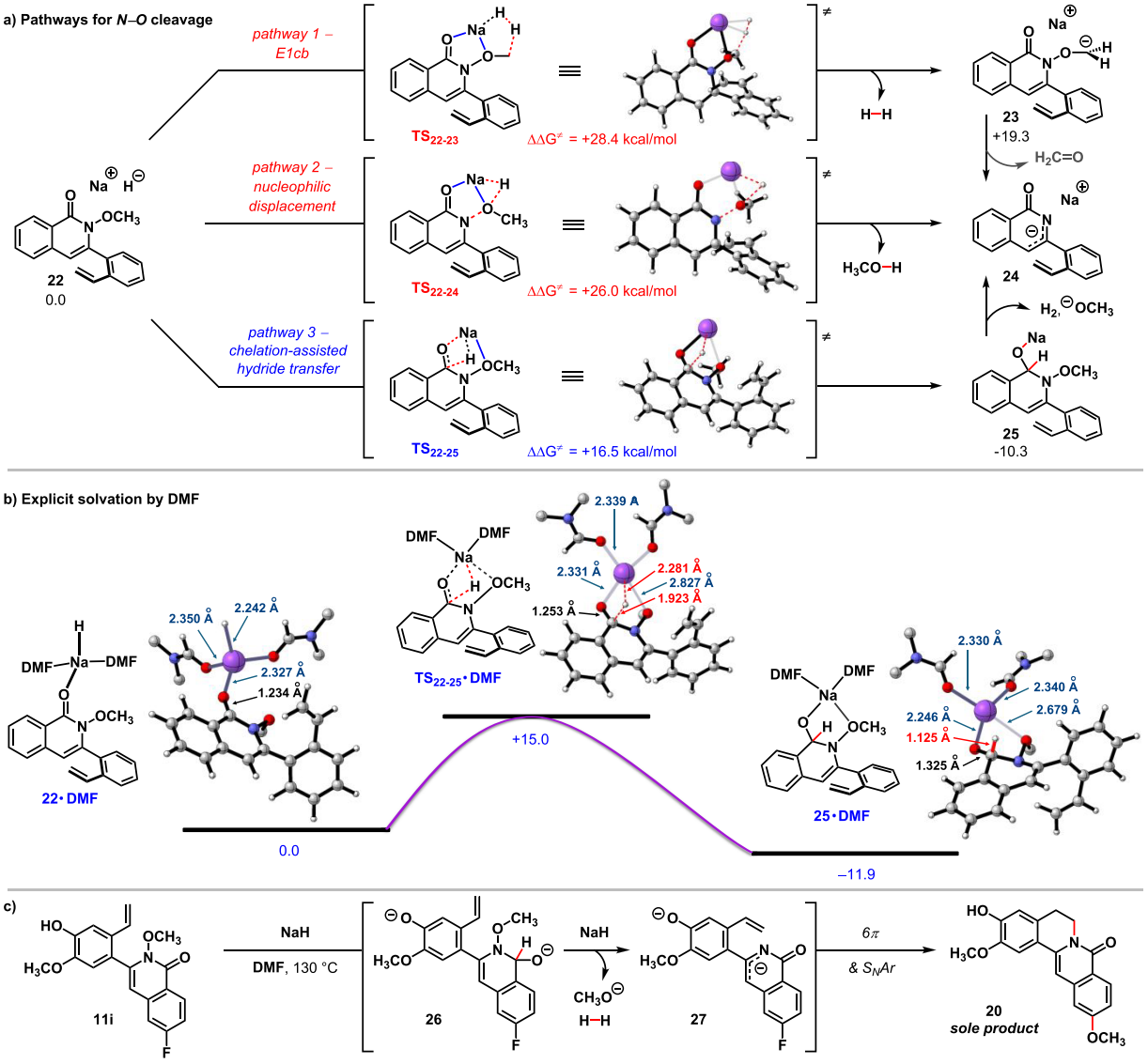

similar inhibitory potential. Rendering the D-ring electron-deficient with a cyano group (e.g., **18**) gave an inactive compound. Stepharotudine-type compounds **4**, **19**, and **20** with guaiacolic A-rings exerted the greatest activities with unnatural **20** displaying an IC_{50} of 2.5 μM. This data suggests that the protoberberine derivatives examined in this study exhibit a distinct mechanism of action compared to berberine (**1**) and can directly inhibit AMPK. Western blot analysis additionally supports the inhibitory activities of the protoberberine analogs against phosphorylated AMPK (Scheme 1d). While 8-oxypseudopalmatine (**3**) was inactive in vitro, it produced the greatest inhibition when subjected to whole cells by Western blot. Presumably, demethylation of one or more of the methoxy substituents in cells generated a guaicolic derivative that exerts greater potency. We were able to test the B-ring distortion analogs (**4-iso** and **20-iso**) by Western blot analysis and found them to also inhibit p-AMPK (see SI). Thus, deviating from planarity does not substantially impact AMPK modulation. Collectively, the data suggest that the A-ring guaiacolic −OH group and an electron-rich D-ring are important in enhancing AMPK inhibition. Our study is the first to uncover the AMPK inhibition potential of protoberberines that have long been studied for their activation properties, while elucidating structural features that govern bioactivity.

2.3. Mechanism of *N*-Deprotection and Aza-6π-Electrocyclization

The *N*-methoxy substituent of the hydroxamic esters (**8**) is important in facilitating directed C−H activation[16] and doubles as an amide protecting group. *N*-Deprotection followed by aza-6π-electrocyclization provide direct and facile entry into the target oxyberberine scaffold. We evaluated three possible mechanistic scenarios by density functional theory (DFT) via Gaussian 16[17] at the B3LYP/6-311+G(2d,p) level of theory,[18−21] including a solvent correction using the CPCM method[22] with dimethylformamide as the solvent (Scheme

https://doi.org/10.1021/jacsau.5c00047
JACS Au 2025, 5, 1429−1438

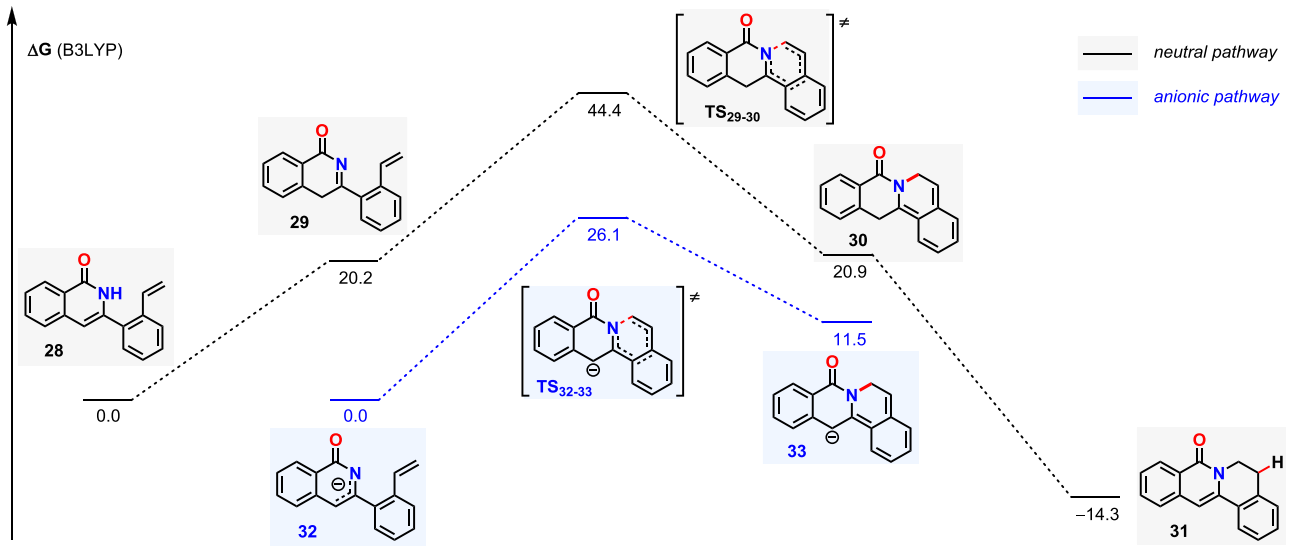

Figure 2. Free energy (kcal/mol) profile for the aza-6π-electrocyclization at the B3LYP/6-311++G(d,p) level of theory with implicit solvation (CPCM) by DMF.

2a). We initially chose to use molecular NaH to approximate energetic barriers in our DFT study because its application in DFT has been reported by Houk,[23] as well as Hirao and Chiba[24] (see SI for an expanded discussion). The pathway where NaH acts as a base, participating in an E1cb elimination reaction via rate-limiting $\mathbf{TS_{22-23}}$ to release conjugate base **23** and formaldehyde as the byproduct (Scheme 2a, pathway 1) occurs with a rate-limiting barrier of 28.4 kcal/mol. Subsequent fragmentation with loss of formaldehyde generates quinolone anion **24** (see SI for full energy diagram and mechanism). If this pathway was operative, we expected to observe side-products originating from Friedel−Crafts reactivity with formaldehyde,[25] especially under high temperature conditions. However, Friedel−Crafts-type products were never detected over the course of our studies. Based on a proposal by Huang and co-workers,[14] we considered a nucleophilic displacement (S_N2-type) reaction by NaH and located a transition state ($\mathbf{TS_{22-24}}$, $\Delta\Delta G^{\ddagger}$ = 26.0 kcal/mol) in which the hydride engages in an S_N2-type fashion to cleave the *N*−*O* bond, directly forming quinolone anion **24** (pathway 2). We posited that NaH can potentially engage the carbonyl in a reduction manner,[24,26] and computed $\mathbf{TS_{22-25}}$ with a significantly lower barrier of 16.5 kcal/mol, to arrive at tetrahedral intermediate **25**, which then collapses ($\Delta\Delta G_{25-24}^{\ddagger}$ = +6.0 kcal/mol, see SI) to the same aromatic anion **24** (pathway 3). Such a nucleophilic hydride transfer by NaH would represent previously undisclosed reduction reactivity occurring under additive-free conditions. Previous DFT calculations to understand NaH-mediated nucleophilicity explicitly included two molecules of solvent ligating sodium[24]; therefore, pathway 3 was also computed via both implicit (CPCM with DMF) and explicit solvation to corroborate our results. The inclusion of two molecules of DMF supporting sodium provided additional stabilization to both the rate-determining hydride-delivery transition state ($\mathbf{TS_{22-25}}$**·DMF**) ($\Delta\Delta G^{\ddagger}$ = 15.0 kcal/mol, Scheme 2b) and the resulting tetrahedral intermediate **25·DMF**. This unusual nucleophilic hydride delivery is likely proceeding under chelation assistance by the *N*-methoxylactam motif and the analogous transition state structure for NaH-mediated hydride transfer to formaldehyde lacking a chelating group could not be located (see SI). When fluorinated *N*-methoxyisoquinolone **11i** was subjected to deprotection/aza-6π-electrocyclization, remote *N*-to-*C* migration of the methoxy group ensued, leading to the isolation of methoxy-substituted oxyberberine **20** as the sole product, presumably through the intermediacy of **26** and **27** (Scheme 2c). Supportive of pathway 3 (Scheme 2a), this outcome is rationalized to occur through a nucleophilic aromatic substitution by the methoxide anion ejected from *N*-deprotection. We note that the NaH-NaI composite system in THF, as developed by Hirao and Chiba,[24,26] does not promote the desired transformation. This suggests that NaH in DMF provides distinct reactivity.

The necessity for base suggests that the anionic attributes of intermediates **12** (Scheme 1a), **24** (Scheme 2a), and **27** (Scheme 2c) may be facilitating the subsequent aza-6π-electrocyclization. While anionic aza-Cope[27] and anionic 4π-electrocyclic[28] reactions have been well-documented in the literature, our study adds to the one other anionic 6π-electrocyclic ring closure that has been previously reported.[29] We computed the Gibbs free energy profiles for both the anionic and neutral pathways by DFT and found the anion acceleration effect to be significant (Figure 2). The barrier to anionic aza-6π-electrocyclization is 18.3 kcal/mol lower in energy compared to the neutral pathway when examining the transition state energies of $\mathbf{TS_{29-30}}$ and $\mathbf{TS_{32-33}}$ ($\Delta\Delta G^{\ddagger}$ = 44.4−26.1 = 18.3 kcal/mol), the origin of which is rationalized to be ground state destabilization akin to the anionic oxy-Cope,[30] carbanionic Claisen,[31] and anionic oxy-Claisen[32] rearrangements. In the present aza-electrocyclization, isomerization of the enamide component of isoquinolone **28** to acylimine **29** is 20.2 kcal/mol uphill by DFT, a consequence that is negated upon deprotonation to anion **32**. In other words, the anionic path effectively bypasses the tautomerization step required in the neutral path. The annulation process to tetracycle **33** is thermodynamically uphill, and the driving force is attributed to protonation by solvent DMF. This and the reversible nature of the electrocyclization is corroborated by experimental mechanistic studies conducted in deuterated DMF (Scheme 3). In most cases, KO*t*-Bu is necessary to effect 6π-electrocyclic ring closure following NaH-mediated *N*−*O* bond cleavage. When cyclization precursor **11d** was subjected

https://doi.org/10.1021/jacsau.5c00047
JACS Au 2025, 5, 1429−1438

Scheme 3. (a) Reversibility in Sequential Deprotection/Aza-6π-Electrocyclization with NaH; (b) Irreversible 6π-Electrocyclization with KO*t*-Bu

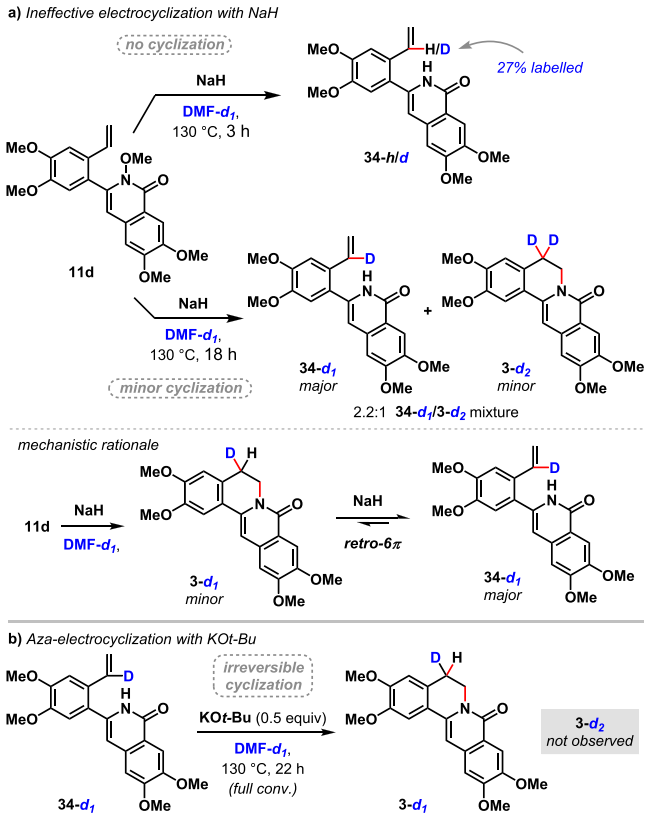

to NaH in deuterated DMF, deprotected isoquinolone **34** was observed as the sole product with 27% deuterium-labeling at the internal site of the alkene (Scheme 3a). Prolonged heating led to a mixture of monodeuterated isoquinolone **34**-d_1 and dideuterated 8- oxypseudopalmatine **3**-d_2 in a 2.2:1 ratio in favor of the acyclic intermediate. Incorporation of deuterium into the alkene is rationalized to occur by aza-6π-electrocyclization, deuteration by DMF-d_1, and base-mediated 6π-electrocyclic ring-opening or elimination. Extended exposure to NaH and heat would promote cyclization to dideuterated **3**-d_2. These observations are consistent with the DFT calculations that suggest aza-electrocyclization to be endergonic. Under KO*t*-Bu catalysis conditions, electrocyclic ring-closure to 8-oxypseudopalmatine **3**-d_1 is irreversible due to KO*t*-Bu's lower basicity (Scheme 3b). In contrast to dideuteration of the tetracycle, only monodeuterated **3**-d_1 is generated from protonation by *t*-BuOH or the isoquinolone that are more acidic than DMF. In essence, substrates involved in thermodynamically uphill reactions will require KO*t*-Bu to drive ring closure to completion because it cannot promote retro-electrocyclization. Past mechanistic studies on reactions involving KO*t*-Bu in DMF generally invoke single-electron transfer pathways[33]; however, the current deprotection/aza-6π-electrocyclization sequence is better consistent with a polar two-electron pathway, proceeding under air, inert atmosphere, and in the presence of TEMPO (see SI). The base-mediated anionic aza-6π-electrocyclization reported herein is distinct from and complementary to the acid-mediated 6π-aza-electrocyclization for benzoquinoline synthesis[34] and C−H alkenylation/6π-electrocyclization cascade for dihydropyridine synthesis.[35]

2.4. Modification of the Protoberberine C-Ring: Restoration of AMPK Activation Activity

Contrary to previous reports of protoberberine synthesis,[8] the present modular and convergent strategy stands out as the sole method capable of modifying all four rings of the tetracyclic scaffold, thereby facilitating the preparation of diverse analogs. Scheme 1a,b show rings A and D being modified by starting with various readily accessible silyl enol ethers **7** and hydroxamic esters **8** as coupling partners. While this study focused on introducing a vinyl group by Suzuki cross-coupling, incorporating substituted alkenes would generate novel B-ring analogs. Distorted B-ring analogs **4-iso** and **20-iso** were formed as minor side products and isolated for bioassays; however, they can be deliberately synthesized by Markovnikov hydration of the vinyl group,[36] followed by cyclization. The oxidative C−H functionalization of *N*-methoxybenzamides with silyl enol ethers was necessary to access natural protoberberines without substitution on the alkene of the C-ring. This strategy is also amenable in employing related C−H functionalization reactions with the broader class of internal alkynes to generate C-ring analogs.[37] This is exemplified in the synthesis of aminoprotoberberine **40** (Scheme 4). The

Scheme 4. C−H Functionalization/Suzuki/Anionic Aza-6π-Electrocyclization Sequence En-Route to Aminoprotoberberine with C-Ring Derivatization

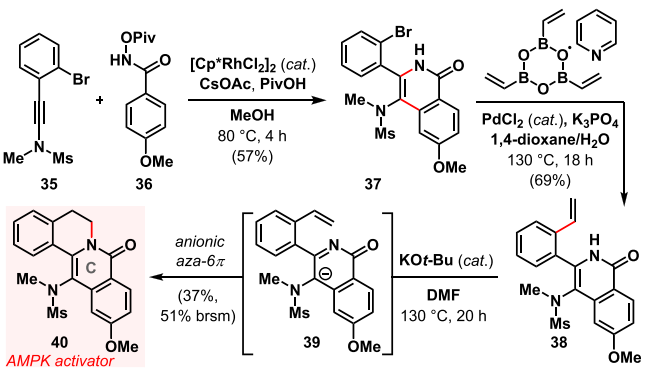

annulative coupling between ynamide **35** and *N*-pivaloylbenzamide **36** yields aminoisoquinolone **37** in 57% yield.[38] Despite the additional sulfonamide group, Suzuki cross-coupling to append on the vinyl substituent proceeds in 69% yield. Since the *N*−*O* bond is cleaved in the C−H functionalization step, aza-6π-electrocyclization can be initiated by treating isoquinolone **38** with catalytic KO*t*-Bu, presumably forming anionic intermediate **39** en-route to the target tetracycle (**40**) in 37% yield (51% brsm). Western blot analysis revealed that C-ring modification with a sulfonamide group restored AMPK activation (see SI).

3. CONCLUSIONS

Utilizing C−H functionalization and anionic aza-6π-electrocyclization strategies developed in our lab, we have orchestrated a concise and convergent strategy that generates diverse protoberberine natural and unnatural products with derivatization at all the A, B, C and D rings. Derivatives with electron-donating groups on the D-ring tend to be unstable to purification. In the process, we have uncovered nucleophilic

https://doi.org/10.1021/jacsau.5c00047
JACS Au 2025, 5, 1429−1438

hydride reactivity elicited by NaH in DMF and in the absence of external additives such as NaI. The natural product stepharotudine (**4**) was synthesized for the first time. Traditionally, protoberberine derivatives have been developed and studied under the presumption that they act as AMPK activators, as evidenced by several studies[2c,6,39] and patents[40] focused on their potential use in treating diabetes. However, our findings challenge this paradigm by demonstrating that many protoberberines are AMPK inhibitors, a previously unappreciated property. This insight opens new avenues for the biomedical relevance of these compounds, particularly in areas where AMPK inhibition could be therapeutically beneficial. Furthermore, we found that incorporating a sulfonamide group into the C-ring restores AMPK activation, providing a novel insight for future explorations of berberine-derived AMPK modulators. There is currently substantial interest in advancing AMPK activators for obesity, diabetes, and liver illnesses, and we envision that the advancement of AMPK inhibitors will have novel therapeutic applications in cancer treatment, controlling autophagy, and elderly wasting.

4. METHODS

4.1. General Procedure for Sequential Rh-Catalyzed C−H Functionalization/Elimination to Generate Isoquinolones 10

To a round-bottom flask under N_2 is added hydroxamic ester **8** (1 equiv), AgOAc (2.2 equiv), $[Cp^*RhCl]_2$ (5 mol %), and THF (0.2 M with respect to **8**). After stirring at rt for 1 min, silyl enol ether **7** (1.2 equiv) is added and the reaction mixture heated at 50 °C for 18 h. The resulting mixture is cooled to rt, filtered through a short plug of silica gel, eluting with CH_2Cl_2 and subsequently EtOAc. The filtrate is concentrated *in vacuo*. The crude 3-hydroxydihydroisoquinolone **9** formed in this manner is resuspended in CH_2Cl_2, briefly treated with concentrated HCl (12 M, 1 equiv), and then concentrated *in vacuo* once more. Purification by silica gel chromatography (eluting with EtOAc/hexanes mixtures) yields multisubstituted isoquinolones **10** in up to 76% yield.

4.2. General Procedure for Ligand-Free Suzuki Coupling Reactions to Furnish 3-Arylisoquinolones 11

A microwave vial or pressure vessel is charged with $PdCl_2$ (5 mol %), aryl halide **10** (1 equiv), and 1,4-dioxane (0.1 M). The resulting mixture is stirred at rt for 20 min, and then added K_3PO_4 (3 equiv), trivinylboroxine pyridine complex (1.5 equiv), and dH_2O (2.2× volume of 1,4-dioxane). The reaction vessel is sealed and heated to 130 °C for 18 h. After cooling to rt, additional H_2O (2.2× volume of 1,4-dioxane) is added, the biphasic mixture separated, and the aqueous layer extracted with CH_2Cl_2 and EtOAc. The combined organic extract is dried over anhydrous Na_2SO_4, filtered, and concentrated *in vacuo*. Purification by silica gel chromatography (eluting with acetone/hexanes mixtures) yields the cross-coupled products (**11**) in up to 98% yields.

4.3. General Procedure for Sequential *N*-Deprotection/Anionic Aza-6π-Electrocyclization to Access Protoberberine Derivatives

In a 1-dram vial, isoquinolone **11** (1 equiv) and NaH (3 equiv) are dissolved in anhydrous DMF (0.1−0.2 M). The vessel is sealed and the mixture heated at 130 °C for 3 h. After cooling, the reaction mixture is concentrated *in vacuo*. The crude *N*-deprotected isoquinoline is resuspended in a solution of KO*t*-Bu (2.5 equiv, prepared as a 0.1 M DMF solution), which is heated at 130 °C for 20 h. The cooled reaction mixture is quenched with dH_2O and extracted with EtOAc. The combined organic extract is washed with brine, dried over anhydrous Na_2SO_4, filtered, and concentrated *in vacuo*. Purification by silica gel chromatography (eluting with EtOAc/hexanes or acetone/hexanes mixtures) yields protoberberine derivatives in up to 84% isolated yields.

4.4. General Procedure for Western Blot Assays

Cell lysates (20 μg) are subjected to electrophoresis on 10% acrylamide gels and transferred to polyvinylidene difluoride (PVDF) membranes. The membranes are incubated for 1 h with blocking buffer (either TBS-T containing 5% [w/v] BSA or 5% skim milk). The membranes are then incubated with the indicated primary antibodies diluted in blocking buffer (1:1,000) for 12 h at 4 °C: anti-pAmpk-α Thr172 (Cell Signaling, #2535s), anti-Ampk-α (Cell Signaling, #2532), and anti-GAPDH (Cell Signaling, #2118). The membranes are washed three times with TBS-T and incubated with the secondary HRP-conjugated antibodies mouse antirabbit IgG-HRP (Cell Signaling, #7074S) (diluted 1:2000 in 5% skim milk) at rt for 1 h. Finally, the membranes are washed in TBS-T three times for 10 min each, and the signal is detected using enhanced chemiluminescence reagent (Pierce, IL, USA). Protein levels are quantified by densitometry using ImageJ software.

4.5. General Procedure for AMPK Kinase Activity Assays

In vitro AMPK kinase assays are performed at Reaction Biology Corporation using the "HotSpot" assay platform.[41] Briefly, SAMStide synthetic peptide substrate (HMRSAMSGLHLVKRR) are prepared in reaction buffer; 20 mM Hepes pH 7.5, 10 mM $MgCl_2$, 1 mM EGTA, 0.02% Brij35, 0.02 mg/mL BSA, 0.1 mM Na_3VO_4, 2 mM DTT, 1% DMSO. AMPK kinase is delivered into the substrate solution and gently mixed. The protoberberine derivatives are delivered into the reaction. After approximately 20 min, a mixture of ATP (Sigma) and ^{33}P ATP (PerkinElmer) is added and made to a final concentration of 10 μM. Reactions are carried out at 25 °C for 120 min, followed by spotting of the reactions onto Whatman grade P81 ion exchange chromatography paper. Unbound phosphate are removed by extensive washing of filters in 0.75% phosphoric acid. After subtraction of the background derived from control reactions containing inactive enzyme, kinase activity data are expressed as the percent remaining kinase activity in test samples compared to vehicle (DMSO) reactions. IC_{50} values and curve fits are obtained using Prism (GraphPad Software).

■ ASSOCIATED CONTENT

Supporting Information

The Supporting Information is available free of charge at https://pubs.acs.org/doi/10.1021/jacsau.5c00047.

Additional experimental details including methods for the preparation of substrates and biological assays, density functional theory (DFT) studies, characterization data, and NMR Spectra (PDF)

■ AUTHOR INFORMATION

Corresponding Authors

Wendong Huang − *Department of Diabetes Complications and Metabolism Research, City of Hope National Medical Center, Duarte, California 91010, United States*; Email: whuang@coh.org

Kevin G. M. Kou − *Department of Chemistry, University of California, Riverside, California 92507, United States*; orcid.org/0000-0002-4676-8846; Email: kevink@ucr.edu

Authors

Yujie Cao − *Department of Chemistry, University of California, Riverside, California 92507, United States*

Justin S. M. Perry − *Department of Chemistry, University of California, Riverside, California 92507, United States*

https://doi.org/10.1021/jacsau.5c00047
JACS Au 2025, 5, 1429−1438

Eryun Zhang − *Department of Diabetes Complications and Metabolism Research, City of Hope National Medical Center, Duarte, California 91010, United States*
Andy Trinh − *Department of Chemistry, University of California, Riverside, California 92507, United States*
Arnav Kacker − *Department of Chemistry, University of California, Riverside, California 92507, United States*
Shayne Cruz − *Department of Chemistry, University of California, Riverside, California 92507, United States*
Hannah Ceballos − *Department of Diabetes Complications and Metabolism Research, City of Hope National Medical Center, Duarte, California 91010, United States*
Aaron Pan − *Department of Chemistry, University of California, Riverside, California 92507, United States*

Complete contact information is available at: https://pubs.acs.org/10.1021/jacsau.5c00047

Author Contributions

[#]J.S.M.P. and E.Z. contributed equally. The manuscript was written through contributions of all authors. CRediT: **Yujie Cao** data curation, formal analysis, investigation, methodology, writing - review & editing; **Justin S. M. Perry** data curation, formal analysis, investigation, methodology, writing - review & editing; **Eryun Zhang** data curation, formal analysis, investigation, methodology, writing - review & editing; **Andy Trinh** data curation, formal analysis, investigation, methodology; **Arnav Kacker** data curation, investigation, methodology; **Shayne Cruz** data curation, investigation, methodology; **Hannah Ceballos** data curation, investigation, methodology; **Aaron Pan** data curation, formal analysis, writing - review & editing; **Wendong Huang** conceptualization, funding acquisition, investigation, project administration, writing - review & editing; **Kevin G. M. Kou** conceptualization, data curation, formal analysis, funding acquisition, investigation, project administration, writing - original draft, writing - review & editing.

Notes

The authors declare the following competing financial interest(s): The authors declare that the novel protoberberine-based AMPK inhibitors described in this study is included in a provisional patent that is jointly owned by the authors and the University of California, Riverside (UCR). The potential financial interest in the patent does not affect the integrity or objectivity of the study. All research findings and conclusions are independent of any financial and intellectual property considerations.

ACKNOWLEDGMENTS

This study was supported in part by the COH-UCR Biomedical Research Initiative, UCOP Cancer Research Coordinating Committee (CRCC Award# C21CR2162), UCR startup funds, the National Institutes of Health (R01DK124627 and R01DK138665 to W.H.), and the National Science Foundation (CAREER Award# 2340731 to K.G.M.K.). S.C. is a MARC Scholar and acknowledges funding through the Maximizing Access to Research Careers (MARC) Trainee Program. The Agilent 6545 Q-TOF LC/MS instrument is funded by NSF grant CHE-1828782. We also thank Beter Zaki and Yaseen Hakim for their early contributions to the synthesis plan.

REFERENCES

(1) (a) Spaulding, H. R.; Yan, Z. AMPK and the Adaptation to Exercise. *Annu. Rev. Physiol.* **2022**, *84*, 209−227. (b) Steinber, G. R.; Carling, D. AMP-activated protein kinase: the current landscape for drug development. *Nat. Rev. Drug Discovery* **2019**, *18*, 527−551.
(2) (a) Pollard, A. E.; Martins, L.; Muckett, P. J.; Khadayate, S.; Bornot, A.; Clausen, M.; Admyre, T.; Bjursell, M.; Fiadeira, R.; Wilson, L.; Whilding, C.; Kotiadis, V. N.; Duchen, M. R.; Sutton, D.; Penfold, L.; Sardini, A.; Bohlooly-Y, M.; Smith, D. M.; Read, J. A.; Snowden, M. A.; Woods, A.; Carling, D. AMPK activation protects against diet induced obesity through Ucp1-independent thermogenesis in subcutaneous white adipose tissue. *Nat. Metab.* **2019**, *1*, 340−349. (b) Liu, Y.; Jurczak, M. J.; Lear, T. B.; Lin, B.; Larsen, M. B.; Kennerdell, J. R.; Chen, Y.; Huckestein, B. R.; Nguyen, M. K.; Tuncer, F.; Jiang, Y.; Monga, S. P.; O'Donnell, C. P.; Finkel, T.; Chen, B. B.; Mallampalli, R. K. A Fbxo48 inhibitor prevents pAMPKα degradation and ameliorates insulin resistance. *Nat. Chem. Bio.* **2021**, *17*, 298−306. (c) Zhang, E.; Jin, L.; Wang, Y.; Tu, J.; Zheng, R.; Ding, L.; Fang, Z.; Fan, M.; Al-Abdullah, I.; Natarajan, R.; Ma, K.; Wang, Z.; Riggs, A. D.; Shuck, S. C.; Yang, L.; Huang, W. Intestinal AMPK modulation of microbiota mediates crosstalk with brown fat to control thermogenesis. *Nat. Commun.* **2022**, *13*, 1135. (d) Steinberg, G. R.; Hardie, D. G. New insights into activation and function of the AMPK. *Nat. Rev. Mol. Cell. Biol.* **2023**, *24*, 255.
(3) (a) Jeon, S.-M.; Chandel, N. S.; Hay, N. AMPK regulates NADPH homeostasis to promote tumour cell survival during energy stress. *Nature* **2012**, *485*, 661−665. (b) Jeon, S.-M.; Hay, N. The double-edged sword of AMPK signaling in cancer and its therapeutic implications. *Arch. Pharm. Res.* **2015**, *38*, 346−357. (c) Dasgupta, B.; Chhipa, R. R. Evolving Lessons on the Complex Role of AMPK in Normal Physiology and Cancer. *Trends Pharmacol. Sci.* **2016**, *37*, 192−206. (d) Eichner, L. J.; Brun, S. N.; Herzig, S.; Young, N. P.; Curtis, S. D.; Shackelford, D. B.; Shokhirev, M. N.; Leblanc, M.; Vera, L. I.; Hutchins, A.; Ross, D. S.; Shaw, R. J.; Svensson, R. U. Genetic Analysis Reveals AMPK Is Required to Support Tumor Growth in Murine Kras-Dependent Lung Cancer Models. *Cell Metab.* **2019**, *29*, 285−302.e7. (e) Sadria, M.; Seo, D.; Layton, A. T. The mixed blessing of AMPK signaling in Cancer treatments. *BMC Cancer* **2022**, *22*, 105.
(4) (a) Whitmarsh-Everiss, T.; Laraia, L. Small molecule probes for targeting autophagy. *Nat. Chem. Biol.* **2021**, *17*, 653−664. (b) Barnaba, C.; Broadbent, D. G.; Kaminsky, E. G.; Perez, G. I.; Schmidt, J. C. AMPK regulates phagophore-to-autophagosome maturation. *J. Cell. Biol.* **2024**, *223*, No. e202309145.
(5) Hardie, D. G. AMPK: a target for drugs and natural products with effects on both diabetes and cancer. *Diabetes* **2013**, *62*, 2164−72.
(6) (a) Cao, S.; Zhou, Y.; Xu, P.; Wang, Y.; Yan, J.; Bin, W.; Qiu, F.; Kang, N. Berberine metabolites exhibit triglyceride-lowering effects via activation of AMP-activated protein kinase in Hep G2 cells. *J. Ethnopharmacol.* **2013**, *149*, 576−582. (b) Zhou, Y.; Cao, S.; Wang, Y.; Xu, P.; Yan, J.; Bin, W.; Qiu, F.; Kang, N. Berberine metabolites could induce low density lipoprotein receptor up-regulation to exert lipid-lowering effects in human hepatoma cells. *Fitoterapia* **2014**, *92*, 230−7.
(7) (a) Le, T. N.; Gang, S. G.; Cho, W.-J. A Versatile Total Synthesis of Benzo[c]phenanthridine and Protoberberine Alkaloids Using Lithiated Toluamide−Benzonitrile Cycloaddition. *J. Org. Chem.* **2004**, *69*, 2768−2772. (b) Van, H. T. M.; Yang, S. H.; Khadka, D. B.; Kim, Y.-C.; Cho, W.-J. Total synthesis of 8-oxypseudopalmatine and 8-oxypseudoberberine via ring-closing metathesis. *Tetrahedron* **2009**, *65*, 10142−10148. (c) Gatland, A. E.; Pilgram, B. S.; Procopiou, P. A.; Donohue, T. J. Short and Efficient Syntheses of Protoberberine Alkaloids using Palladium-Catalyzed Enolate Arylation. *Angew. Chem., Int. Ed.* **2014**, *53* (52), 14555−14558. *Angew. Chem.* **2014**, *126*, 14783−14786, 10.1002/ange.201409164. (d) Jayakumar, J.; Cheng, C.-H. Direct Synthesis of Protoberberine Alkaloids by Rh-Catalyzed C−H Bond Activation as the Key Step. *Chem. − Eur. J.* **2016**, *22* (5), 1800−1804. (e) Zhou, S.; Tong, R. A General, Concise Strategy that Enables Collective Total Syntheses of over 50

Protoberberine and Five Aporhoeadane Alkaloids within Four to Eight Steps. *Chem. – Eur. J.* **2016**, *22* (21), 7084–7089. (f) Li, S.; Nie, H.; Duan, M.; Wang, W.; Zhu, C.; Song, C. Construction of a Protoberberine Alkaloid Skeleton via the Palladium-Catalyzed α-Arylation–Amide Formation Cascade. *Org. Lett.* **2021**, *23* (24), 9631–9634. (g) Tajiri, M.; Yamada, R.; Hotsumi, M.; Makabe, K.; Konno, H. The total synthesis of berberine and selected analogues, and their evaluation as amyloid beta aggregation inhibitors. *Eur. J. Med. Chem.* **2021**, *215*, No. 113289. (h) Sun, Z.; Zhang, X.; Fu, J.; Zhang, L.; Cheng, M.; Yang, L.; Liu, Y. Collective Syntheses of 8-Oxoprotoberberines via Sequential $In(OTf)_3$-Catalyzed Cyclization and $Pd(OAc)_2$-Catalyzed Heck Coupling. *J. Org. Chem.* **2023**, *88* (11), 7179–7187. (i) Song, Y.; Li, R.; Bai, J.; Li, X.; Zhou, S.; Zhang, Y. Carboxylic Acid-Enabled Vinylene Transfer Reaction by Co(III) Catalyst: Scope and Applications to the Five-Step Total Synthesis of Protoberberine Alkaloids Containing Free Hydroxyl Group without Protection. *J. Org. Chem.* **2024**, *89* (5), 3238–3250.

(8) Kou, X.; Kou, K. G. M. α-Arylation of Silyl Enol Ethers via Rhodium(III)-Catalyzed C–H Functionalization. *ACS Catal.* **2020**, *10* (5), 3103–3109.

(9) Cao, Y.; Kou, K. G. M. In *Handbook of C–H Functionalization*, 1st ed.; Maiti, D., Ed.; Rhodium-Catalyzed Heterocycle Synthesis by C–H Functionalization; John Wiley & Sons, Ltd: 2022; pp 1–39.

(10) Xu, M. Y.; Yang, C.; Jiang, W. T.; Xiao, B. Synthesis and Application of Heterocyclic Germatranes via Rhodium-Catalyzed Directed C–H Activation/Annulation with Alkynyl Germatranes and Palladium-Catalyzed Cross-Coupling. *Adv. Synth. Catal.* **2020**, *362* (8), 1706–1711.

(11) Barber, J. S.; Kong, D.; Li, W.; McAlpine, I. J.; Nair, S. K.; Sakata, S. K.; Sun, N.; Patman, R. L. Rhodium(III)-Catalyzed C–H Activation: Annulation of Petrochemical Feedstocks for the Construction of Isoquinolone Scaffolds. *Synlett* **2021**, *32*, 202–206.

(12) Menéndez-Rodríguez, L.; Tomás-Mendivil, E.; Francos, J.; Nájera, C.; Crochet, P.; Cadierno, V. Palladium(II) complexes with a phosphino-oxime ligand: synthesis, structure and applications to the catalytic rearrangement and dehydration of aldoximes. *Catal. Sci. Technol.* **2015**, *5*, 3754–3761.

(13) Barcan, G. A.; Patel, A.; Houk, K. N.; Kwon, O. A Torquoselective 6π Electrocyclization Approach to Reserpine Alkaloids. *Org. Lett.* **2012**, *14* (21), 5388–5391.

(14) Lu, S.; Lin, Y.; Zhong, H.; Zhao, K.; Huang, J. A practical one-pot procedure for the synthesis of N–H isoquinolones. *Tetrahedron Lett.* **2013**, *54* (15), 2001–2005.

(15) (a) Huigens, R. W., III; Morrison, K. C.; Hicklin, R. W.; Flood, T. A., Jr; Richter, M. F.; Hergenrother, P. J. A ring-distortion strategy to construct stereochemically complex and structurally diverse compounds from natural products. *Nat. Chem.* **2013**, *5*, 195–202. (b) Li, Y.; Cheng, S.; Tian, Y.; Zhang, Y.; Zhao, Y. Recent ring distortion reactions for diversifying complex natural products. *Nat. Prod. Rep.* **2022**, *39* (10), 1970–1992.

(16) Zhu, R.-Y.; Farmer, M. E.; Chen, Y.-Q.; Yu, J.-Q. A Simple and Versatile Amide Directing Group for C–H Functionalizations. *Angew. Chem., Int. Ed.* **2016**, *55* (36), 10578–10599.

(17) Frisch, M. J.; Trucks, G. W.; Schlegel, H. B.; Scuseria, G. E.; Robb, M. A.; Cheeseman, J. R.; Scalmani, G.; Bar-one, V.; Petersson, G. A.; Nakatsuji, H.; Li, X.; Caricato, M.; Marenich, A. V.; Bloino, J.; Janesko, B. G.; Gomperts, R.; Mennucci, B.; Hratchian, H. P.; Ortiz, J. V.; Izmaylov, A. F.; Sonnenberg, J. L.; Williams-Young, D.; Ding, F.; Lipparini, F.; Egidi, F.; Goings, J.; Peng, B.; Petrone, A.; Henderson, T.; Ranasinghe, D.; Zakrzewski, V. G.; Gao, J.; Rega, N.; Zheng, G.; Liang, W.; Hada, M.; Ehara, M.; Toyota, K.; Fukuda, R.; Hasegawa, J.; Ishida, M.; Nakajima, T.; Honda, Y.; Kitao, O.; Nakai, H.; Vreven, T.; Throssell, K.; Montgom-ery, J. A., Jr.; Peralta, J. E.; Ogliaro, F.; Bearpark, M. J.; Heyd, J. J.; Brothers, E. N.; Kudin, K. N.; Staroverov, V. N.; Keith, T. A.; Koba-yashi, R.; Normand, J.; Raghavachari, K.; Rendell, A. P.; Burant, J. C.; Iyengar, S. S.; Tomasi, J.; Cossi, M.; Millam, J. M.; Klene, M.; Adamo, C.; Cammi, R.; Ochterski, J. W.; Martin, R. L.; Morokuma, K.; Farkas, O.; Foresman, J. B.; Fox, D. J. *Gaussian 16, Revision C.01*; Gsussian, Inc.: Wallingford, CT, 2016.

(18) Becke, A. D. Density-Functional Thermochemistry. III. The Role of Exact Exchange. *J. Chem. Phys.* **1993**, *98*, 5648–5652.

(19) Lee, C.; Yang, W.; Parr, R. G. Development of the Colle-Salvetti correlation-energy formula into a functional of the electron density. *Phys. Rev. B* **1988**, *37*, 785–789.

(20) Vosko, S. H.; Wilk, L.; Nusair, M. Accurate spin-dependent electron liquid correlation energies for local spin density calculations: a critical analysis. *Can. J. Phys.* **1980**, *58*, 1200–1211.

(21) Stephens, P. J.; Devlin, F. J.; Chabalowski, C. F.; Frisch, M. J. Ab Initio Calculation of Vibrational Absorption and Circular Dichroism Spectra Using Density Functional Force Fields. *J. Phys. Chem.* **1994**, *98*, 11623–11627.

(22) Takano, Y.; Houk, K. N. Benchmarking the Conductor-like Polarizable Continuum Model (CPCM) for Aqueous Solvation Free Energies of Neutral and Ionic Organic Molecules. *J. Chem. Theory Comput.* **2005**, *1*, 70–77.

(23) Wu, Y.-D.; Tucker, J. A.; Houk, K. N. Stereoselectivities of Nucleophilic Additions to Cyclohexanones Substituted by Polar Groups. Experimental Investigation of Reductions of *trans*-Decalones and Theoretical Studies of Cyclohexanone Reductions. The Influence of Remote Electrostatic Effects. *J. Am. Chem. Soc.* **1991**, *113*, 5018–5027.

(24) Ong, D. Y.; Tejo, C.; Xu, K.; Hirao, H.; Chiba, S. Hydrodehalogenation of Haloarenes by a Sodium Hydride-Iodide Composite. *Angew. Chem., Int. Ed.* **2017**, *56*, 1840–1844.

(25) (a) Sun, H.-B.; Hua, R.; Yin, Y. An efficient synthesis of diarylmethanes via $InCl_3{\cdot}4H_2O$-catalyzed dehydration of electron-rich arenes with trioxane. *Tetrahedron Lett.* **2006**, *47*, 2291–2294. (b) Li, Z. X.; Duan, Z.; Wu, Y. J. $FeCl_3$ catalyzed diarylmethanes formations. *Chin. Chem. Lett.* **2009**, *20*, 511–513. (c) Crowley, R., III; Lujan, B.; Martinez, A.; Manasi, R.; DeBow, J. D.; Kou, K. G. M. A Fenton Approach to Aromatic Radical Cations and Diarylmethane Synthesis. *J. Org. Chem.* **2023**, *88*, 15060–15066.

(26) (a) Too, P. C.; Chan, G. H.; Tnay, Y. L.; Hirao, H.; Chiba, S. Hydride Reduction by a Sodium Hydride-Iodide Composite. *Angew. Chem., Int. Ed.* **2016**, *55* (11), 3719–3723. *Angew. Chem.* **2016**, *128* (11), 3783–3787, 10.1002/ange.201600305. (b) Hong, Z.; Ong, D. Y.; Muduli, S. K.; Too, P. C.; Chan, G. H.; Tnay, Y. L.; Chiba, S.; Nishiyama, Y.; Hirao, H.; Soo, H. S. Understanding the origins of nucleophilic hydride reactivity of a sodium hydride-iodide composite. *Chem. – Eur. J.* **2016**, *22*, 7108–7114.

(27) (a) Das, P.; Delost, M. D.; Quresh, M. H.; Bao, J.; Fell, J. S.; Houk, K. N.; Njardarson, J. T. Dramatic Effect of γ-Heteroatom Dienolate Substituents on Counterion Assisted Asymmetric Anionic Amino-Cope Reaction Cascades. *J. Am. Chem. Soc.* **2021**, *143* (15), 5793–5804. (b) Qureshi, M. H.; Njardarson, J. T. Anionic Amino-Cope Rearrangement Cascade Synthesis of 2,4-Substituted Benzoate Esters from Acyclic Building Blocks. *Org. Lett.* **2022**, *24* (43), 7978–7982.

(28) (a) Kametani, T.; Tsubuki, M.; Nemoto, H.; Suzuki, K. Concerted ring-opening reaction of cyclobutenes. The extraordinary accelerating effects of arylsulfoxy and sulfonyl carbanion substituents. *J. Am. Chem. Soc.* **1981**, *103* (5), 1256–1258. (b) Paquette, L. A. Cascade Rearrangements Following Twofold Addition of Alkenyl Anions to Squarate Esters. *Eur. J. Org. Chem.* **1998**, *1998* (9), 1709–1728. (c) Paquette, L. A.; Geng, F. Applications of the Squarate Ester Cascade to the Expeditious Synthesis of Hypnophilin, Coriolin, and Ceratopicanol. *J. Am. Chem. Soc.* **2002**, *124* (31), 9199–9203.

(29) Yamaguchi, A. D.; Chepiga, K. M.; Yamaguchi, J.; Itami, K.; Davies, H. M. L. Concise Syntheses of Dictyodendrins A and F by a Sequential C–H Functionalization Strategy. *J. Am. Chem. Soc.* **2015**, *137*, 644–647.

(30) (a) Evans, D. A.; Golob, A. M. [3,3]Sigmatropic rearrangements of 1,5-diene alkoxides. Powerful accelerating effects of the alkoxide substituent. *J. Am. Chem. Soc.* **1975**, *97* (16), 4765–4766. (b) Evans, D. A.; Baillargeon, D. J. Alkoxide substituent effects on carbon—carbon bond homolysis. *Tetrahedron Lett.* **1978**, *19* (36), 3319–3322. (c) Steigerwald, M. L.; Goddard, W. A., III; Evans, D. A.

https://doi.org/10.1021/jacsau.5c00047
JACS Au 2025, 5, 1429–1438

Theoretical studies of the oxy anionic substituent effect. *J. Am. Chem. Soc.* **1979**, *101* (8), 1994−1997.
(31) (a) Denmark, S. E.; Harmata, M. A. Carbanion-Accelerated Claisen Rearrangements. *J. Am. Chem. Soc.* **1982**, *104*, 4972−4974. (b) Denmark, S. E.; Harmata, M. A. Carbanion-accelerated Claisen rearrangements. 2. Studies on internal asymmetric induction. *J. Org. Chem.* **1983**, *48* (19), 3369−3370. (c) Denmark, S. E.; Harmata, M. A. Carbanion-accelerated Claisen rearrangements 3. Vicinal quaternary centers. *Tetrahedron Lett.* **1984**, *25*, 1543.
(32) Koreeda, M.; Luengo, J. I. The anionic oxy-Claisen rearrangement of enolates of alpha-allyloxy ketones. A remarkable rate accelerating effect exhibited by the nature of the counterion. *J. Am. Chem. Soc.* **1985**, *107* (19), 5572−5573.
(33) (a) Drapeau, M. P.; Fabre, I.; Grimaud, L.; Ciofini, I.; Ollevier, T.; Taillefer, M. Transition-Metal-Free α-Arylation of Enolizable Aryl Ketones and Mechanistic Evidence for a Radical Process. *Angew. Chem., Int. Ed.* **2015**, *54* (36), 10587−10591. (b) Chen, Y.-Y.; Zhang, N.-N.; Ye, L.-M.; Chen, J.-H.; Sun, X.; Zhang, Z.-J.; Yan, M. KOt-Bu/DMF promoted intramolecular cyclization of 1,1′-biphenyl aldehydes and ketones: an efficient synthesis of phenanthrenes. *RSC Adv.* **2015**, *5*, 48046−48049. (c) Barham, J. P.; Coulthard, G.; Emery, K. J.; Doni, E.; Cumine, F.; Nocera, G.; John, M. P.; Berlouis, L. E. A.; McGuire, T.; Tuttle, T.; Murphy, J. A. KO*t*Bu: A Privileged Reagent for Electron Transfer Reactions? *J. Am. Chem. Soc.* **2016**, *138*, 7402−7410.
(34) Jiang, X.; Zeng, Z.; Hua, Y.; Xu, B.; Shen, Y.; Xiong, J.; Qiu, H.; Wu, Y.; Hu, T.; Zhang, Y. Merging C−H Vinylation with Switchable 6π-Electrocyclizations for Divergent Heterocycle Synthesis. *J. Am. Chem. Soc.* **2020**, *142* (36), 15585−15594.
(35) Dongbang, S.; Confair, D. N.; Ellman, J. A. Rhodium-Catalyzed C−H Alkenylation/Electrocylization Cascade Provides Dihydropyridines That Serve as Versatile Intermediates to Diverse Nitrogen Heterocycles. *Acc. Chem. Res.* **2021**, *54* (7), 1766−1778.
(36) Cadot, C.; Dalko, P. I.; Cossy, J.; Ollivier, C.; Chuard, R.; Renaud, P. Free-Radical Hydroxylation Reactions of Alkylboronates. *J. Org. Chem.* **2002**, *67* (21), 7193−7202.
(37) (a) Guimond, N.; Gouliaras, C.; Fagnou, K. Rhodium(III)-Catalyzed Isoquinolone Synthesis: The N−O Bond as a Handle for C−N Bond Formation and Catalyst Turnover. *J. Am. Chem. Soc.* **2010**, *132* (20), 6908−6909. (b) Hyster, T. K.; Rovis, T. Rhodium-Catalyzed Oxidative Cycloaddition of Benzamides and Alkynes via C−H/N−H Activation. *J. Am. Chem. Soc.* **2010**, *132* (30), 10565−10569.
(38) Niu, B.; Liu, R.; Wei, Y.; Shi, M. Catalyst-controlled synthesis of 4-amino-isoquinolin-1(2H)-one and oxazole derivatives. *Org. Chem. Front.* **2018**, *5*, 1466−1470.
(39) Yin, Y.; Xing, H.; Ye, J. Efficacy of berberine in patients with type 2 diabetes mellitus. *Metab., Clin. Exp.* **2008**, *57*, 712−717.
(40) (a) Singh, I. P.; Mahajan, S. Berberine and its derivatives: a patent review (2009 - 2012). *Expert Opin. Ther. Pat.* **2013**, *23*, 215−231. (b) Lowery, R.; Wilson, J.; Wells, S.; LaCore, T. Administration of Berberine Metabolites. Patent No. US 10,278,961 B2, May 7, 2019.
(41) Anastassiadis, T.; Deacon, S. W.; Devarajan, K.; Ma, H.; Peterson, J. R. Comprehensive assay of kinase catalytic activity reveals features of kinase inhibitor selectivity. *Nat. Biotechnol.* **2011**, *29*, 1039−1045.

https://doi.org/10.1021/jacsau.5c00047
JACS Au 2025, 5, 1429−1438